Electrochemical Materials and Technologies

ARTICLE

Electrochemical Materials and Technologies

eISSN:2949-0561

Cite this: Electrochem. Mater. Technol. 5 (2026) 20265070

Corrosion inhibition behaviour of clove (*Syzygium aromaticum*) oil extract for mild steel in simulated seawater

Maureen Olere Oisakede [a *], Blessed Osayemwen Enagbonma [a], George Ochuko Emoghene [a], Judith Efionayi [a], Great Chukwudaro Onyejerue [a]

Received: 16 April 2026
Accepted: 5 June 2026
Published online: 17 June 2026

DOI: 10.15826/elmattech.2026.5.070

The corrosion inhibition performance of clove (*Syzygium aromaticum*) essential oil as a green inhibitor for mild steel in simulated seawater was investigated using a combination of electrochemical and surface analytical techniques. Fourier transform infrared (FTIR) spectroscopy confirmed the presence of key phytochemical constituents in the clove extract responsible for inhibitor–metal interactions. Open circuit potential (OCP) measurements demonstrated a stabilizing effect of the extract on the mild steel electrode, indicative of adsorption-driven surface protection. The potentiodynamic polarization (Tafel) analysis revealed a mixed-type inhibition mechanism, with corrosion current densities decreasing from $2.287 \cdot 10^{-6}$ A/cm^2 (control) to as low as $0.887 \cdot 10^{-6}$ A/cm^2 at 3.0 mL/L clove extract, corresponding to a maximum inhibition efficiency of 61.22 % and a reduction in corrosion rate from $2.65 \cdot 10^{-8}$ mm/year to $1.03 \cdot 10^{-8}$ mm/year. Electrochemical impedance spectroscopy (EIS) using Nyquist and Bode plots further corroborated the formation of a protective adsorption layer at the metal–electrolyte interface, consistent with an increase in charge-transfer resistance in the presence of the inhibitor. Scanning electron microscopy (SEM) at magnifications of 500x, 1000x, and 2000x revealed a progressive improvement in surface morphology with increasing inhibitor concentration, with treated specimens exhibiting markedly reduced surface degradation compared to uninhibited controls. Energy dispersive X-ray spectroscopy (EDS) elemental analysis confirmed the incorporation of oxygen-containing species and trace elements on treated surfaces, consistent with protective film formation. These findings collectively demonstrate that clove essential oil is a promising, eco-friendly corrosion inhibitor for mild steel in simulated seawater conditions, offering significant potential for sustainable corrosion management applications.

keywords: clove oil, green corrosion inhibitor, mild steel, simulated seawater, surface morphology

© 2026, the Authors. This article is published in open access under the terms and conditions of the Creative Commons Attribution (CC BY) license (http://creativecommons.org/licenses/by/4.0/).

1. Introduction

Corrosion represents one of the most pervasive and economically devastating challenges confronting modern industry and infrastructure, defined as the electrochemical or chemical deterioration of metals upon interaction with their surrounding environment, imposing enormous financial, structural, and safety burdens across virtually every industrial sector [1]. The landmark International Measures of Prevention, Application, and Economics of Corrosion Technologies (IMPACT) study conducted by NACE International estimated the global annual cost of corrosion at approximately US$2.5 trillion, equivalent to 3.4 % of the world's gross domestic product (GDP), a figure that underscores the extraordinary magnitude of the problem [2]; critically, the same study concluded that the implementation of existing best-practice corrosion control strategies could yield annual savings of between US$375 billion and US$875 billion, demonstrating that a substantial proportion of these losses are preventable [2]. Beyond direct economic losses, corrosion compromises structural integrity, precipitates catastrophic infrastructure failures, and poses significant environmental and public safety risks; in the water infrastructure sector alone, corrosion is responsible for over 260000 pipe failures annually in North America, costing in excess of US$2.6 billion in repair expenditure [3].

a: Department of Materials and Metallurgical Engineering, University of Benin, Benin City 300001, Nigeria

* Corresponding author: maureen.oisakede@uniben.edu

The problem is especially acute in marine and coastal environments, where the combination of dissolved chloride ions, dissolved oxygen, biological activity, variable *p*H, and temperature fluctuations creates a uniquely aggressive corrosive milieu [4, 5]. Mild steel (low-carbon steel), the most widely employed structural material globally, is extensively deployed in shipbuilding, offshore oil and gas platforms, submarine pipelines, harbour structures, marine vessels, and coastal infrastructure due to its favourable mechanical properties, ease of fabrication, and relatively low cost [6]; however, it is inherently susceptible to corrosion in seawater, where anodic dissolution is facilitated by cathodic oxygen reduction reactions at its surface [7, 8].

Corrosion inhibitors – chemical compounds added to a corrosive medium to reduce the rate of metal dissolution – represent one of the most practical and cost-effective approaches to corrosion control [9]. Conventional synthetic inhibitors, including chromates, phosphates, nitrites, and azole-based compounds, have historically provided high inhibition efficiencies through the formation of protective barrier films, the modification of electrochemical reactions, or the alteration of the corrosive environment, typically by virtue of electron-rich functional groups, including nitrogen, oxygen, sulfur, and phosphorus atoms together with aromatic or heterocyclic rings and π-conjugated systems that facilitate adsorptive interaction with the metal surface through coordinative dative covalent bonding [10, 11]. However, their industrial deployment is increasingly constrained by significant environmental and toxicological drawbacks: chromate-based inhibitors are acutely toxic, mutagenic, and carcinogenic and subject to stringent regulatory restrictions [10, 12]; phosphate-based formulations contribute to eutrophication of aquatic systems; and many nitrogen-containing synthetic inhibitors exhibit non-biodegradable behaviour, persisting in marine ecosystems [11, 13]. This regulatory and environmental pressure has catalysed a vigorous global research effort to identify sustainable, environmentally benign alternatives [12, 14].

Plant-derived extracts and essential oils have emerged as a compelling class of sustainable, biodegradable, and eco-friendly corrosion inhibitors, attracting growing scientific attention over the past decade due to their derivation from renewable biological resources, inherent biodegradability and low toxicity, wide availability, and structural diversity of bioactive organic molecules [13–16]. These phytochemical formulations contain a rich array of bioactive compounds – including polyphenols, tannins, flavonoids, alkaloids, terpenoids, and glycerides – possessing the structural prerequisites for effective metal surface adsorption, namely heteroatoms with lone-pair electrons and aromatic π-systems [15, 16]. Research in diverse plant species has consistently demonstrated concentration-dependent inhibition efficiency, with the Langmuir adsorption isotherm frequently identified as the dominant adsorption model, indicating monolayer formation on the metal surface [15]. Electrochemical studies employing potentiodynamic polarization, EIS, and OCP measurements have confirmed that plant extracts most commonly act as mixed-type inhibitors – simultaneously suppressing anodic dissolution and cathodic reduction reactions – and SEM/EDS surface characterisation has provided direct morphological evidence of the protective films deposited on metal surfaces [13, 15, 17].

Among the essential oils of particular interest, those from the Myrtaceae family and specifically from clove (Syzygium aromaticum) have demonstrated exceptional promise due to their extraordinarily high content of electrochemically active phytochemicals [18, 19]. Clove essential oil is chemically dominated by eugenol (4-allyl-2-methoxyphenol), a phenylpropanoid compound constituting between 70 % and 90 % of the total volatile fraction, with eugenyl acetate, β-caryophyllene, and α-humulene as principal secondary constituents [20, 21, 22]. The molecular architecture of eugenol – comprising a guaiacol aromatic scaffold bearing an allyl side-chain, a conjugated π-electron system, an oxygen-bearing methoxy group, a free hydroxyl group, and a terminal alkene moiety – collectively supplies both lone-pair electron donors and π-electron centres capable of adsorptive interaction with the electron-deficient *d*-orbitals of iron via coordinative bonding [18, 19]. Density functional theory (DFT) computations and molecular dynamics simulations have further confirmed that eugenol and β-caryophyllene form stable surface complexes with Fe atoms through oxygen lone-pair donation accompanied by back-donation from filled metal orbitals to the inhibitor's antibonding molecular orbitals [18].

Empirical electrochemical investigations have validated the inhibitory efficacy of Syzygium aromaticum and its principal constituents across multiple corrosive media. Investigations of clove essential oil on mild steel in 0.5 M HCl recorded inhibition efficiencies of up to 94 % at 4 g/L, classifying the oil as a mixed-type inhibitor [18]. Eugenol and its derivative acetyleugenol demonstrated a maximum inhibition efficiency of 91 % at 0.174 g/L in 1 M HCl following Langmuir adsorption behaviour [23]. In chloride-containing media more relevant to marine service, eugenol encapsulated within organoclay composites achieved an inhibition efficiency of 83 %

against brass corrosion in 3 % NaCl with cathodic inhibitor characteristics, and polymerised eugenol as a macromolecular green inhibitor yielded efficiencies of 82–84 % against carbon steel in 1 M HCl [24]. Most recently, polymerised eugenol coatings derived from S. aromaticum were reported to reduce the corrosion rate of carbon steel by 69 % while simultaneously exhibiting antimicrobial activity against E. coli and S. aureus, a dual-functionality attribute of considerable relevance to marine biofouling applications [25].

Despite this growing body of evidence, the application of clove essential oil as a corrosion inhibitor for mild steel in simulated seawater remains comparatively underexplored. The majority of published studies have examined clove oil inhibition in acidic media (HCl, H_2SO_4) or neutral saline solutions at relatively high inhibitor concentrations, with few deploying the comprehensive suite of electrochemical and surface characterisation methodologies required to fully elucidate inhibition mechanisms under marine-relevant conditions [15, 17]. Motivated by the urgent need for non-toxic corrosion mitigation strategies in marine environments and by the demonstrated but incompletely characterised inhibition potential of plant-derived essential oils, the present study investigates the efficacy of Syzygium aromaticum (clove) essential oil as a green corrosion inhibitor for mild steel immersed in simulated seawater. A comprehensive multi-technique characterisation approach is employed, encompassing FTIR spectroscopic analysis, open-circuit potential (OCP) temporal monitoring, potentiodynamic polarization (Tafel) analysis, electrochemical impedance spectroscopy (EIS), and SEM/EDS surface morphological and elemental analysis at three inhibitor concentrations (1.0, 2.0, and 3.0 mL/L) against an uninhibited control.

2. Methodology

2.1. Preparation of mild steel specimens

Mild steel coupons conforming to ASTM A36 specification were used for the electrochemical corrosion studies. [26, 27]. Coupons with dimensions 20 × 15 × 2 mm and an exposed surface area of 4 cm^2 were prepared. The specimens were mechanically polished successively with 300–1200 grit silicon carbide abrasive papers, rinsed thoroughly with distilled water, degreased with ethanol, ultrasonically cleaned, dried in warm air, and stored in a desiccator prior to electrochemical testing to prevent premature oxidation.

2.2. Preparation of simulated seawater

Simulated seawater was prepared using analytical-grade salts at ionic compositions according to ASTM D1141-98 (2013) to ensure controlled and reproducible marine-like corrosivity [28]. To maintain a salinity level of approximately 3.5 %, 35 grammes of analytical-grade sodium chloride (NaCl) were dissolved in one litre of distilled water. In addition to NaCl, trace amounts of magnesium chloride ($MgCl_2$), calcium chloride ($CaCl_2$), potassium chloride (KCl), and sodium sulphate (Na_2SO_4) were incorporated to approximate the ionic complexity of seawater. The *p*H of the solution was measured using a calibrated *p*H metre and adjusted to the range of 7.8–8.3, which corresponds to typical oceanic conditions. The prepared simulated seawater was thoroughly mixed and stored in a sealed container prior to use in corrosion studies. It should be noted that the solution described represents a simplified saline medium inspired by ASTM D1141-98 rather than a full implementation of that standard; exact constituent masses used were: NaCl 35.00 g/L, $MgCl_2$ 5.00 g/L, Na_2SO_4 4.09 g/L, $CaCl_2$ 1.16 g/L, and KCl 0.75 g/L, dissolved in distilled water and *p*H-adjusted to 7.8–8.3.

2.3. Extraction of clove oil

Dried clove buds (Syzygium aromaticum) were finely ground using a mechanical grinder to increase surface area and enhance solvent interaction. A 200 g sample of powdered clove buds was mixed with 2 L of ethanol as the extraction solvent. The mixture was placed on a magnetic stirrer and continuously stirred for approximately two hours at ambient temperature to facilitate extraction of essential oil constituents, such as eugenol and other phenolic compounds responsible for corrosion inhibition. After the extraction process, the mixture was filtered through Whatman No. 1 filter paper to separate the solid residues from the liquid extract. The filtrate (ethanol–clove oil mixture) was then subjected to evaporation in a water bath to remove the ethanol solvent, leaving the clove oil extract behind. The extracted clove oil extract was collected and stored in airtight bottles at room temperature until required for inhibitor preparation.

2.4. Preparation of the test solutions

Clove essential oil was introduced into 100 mL of simulated seawater at concentrations of 1.0 mL/L, 2.0 mL/L, and 3.0 mL/L respectively. An uninhibited blank solution without clove oil served as a control.

2.5. Fourier-transform infrared spectroscopy (FTIR)

Fourier-transform infrared spectroscopy (FTIR) was conducted on the pure clove extract to identify key functional groups present in organic molecules using a mid-IR spectrometer in the 4000–400 cm^{-1} range,

interpreted according to established vibrational assignments for eugenol-rich plant oils [29, 30].

2.6. Electrochemical measurements

The extract was stirred magnetically for 15 minutes to ensure a uniform dispersion of the inhibitor throughout the simulated seawater. During electrochemical testing, the mild steel working electrode was mounted vertically at the centre of the electrochemical cell to minimise direct interaction with any undispersed oil droplets that could accumulate at the bottom of the cell. The electrode was immersed only after complete mixing of the electrolyte, and care was taken to avoid pre-wetting of the steel surface by any floating or sedimented oil phase. Prior to each experiment, the solution was gently stirred to maintain inhibitor homogeneity without introducing significant hydrodynamic effects. These precautions ensured reliable and reproducible electrochemical measurements. The electrochemical behaviour of mild steel in the test media was studied using a potentiostat connected to a conventional three-electrode corrosion cell. The mild steel specimen served as the working electrode, a platinum wire as the counter electrode, and a saturated calomel electrode (SCE) as the reference electrode.

2.6.1. Open circuit potential (OCP)

Each sample was immersed in its respective test solution, and the open circuit potential was monitored over time for 300 s. Stability was assessed visually from the potential-time profile. The OCP evolution indicated the corrosion tendency of the metal surface.

2.6.2. Linear polarisation resistance (LPR)

The LPR test was conducted by polarising the working electrode slightly (± 10–20 mV) about its OCP. The corresponding current response was recorded, and the polarisation resistance (R_p) was determined from the slope of the potential–current plot. A higher R_p value indicates greater corrosion resistance.

2.6.3. Tafel polarisation measurement

Tafel polarisation curves were obtained by sweeping the potential from approximately –250 mV to + 250 mV relative to the OCP at a scan rate of 1 mV/s in the anodic direction. The corrosion potential (E_{corr}) and corrosion current density (i_{corr}) were derived by Tafel extrapolation of the linear portions of the anodic and cathodic Tafel branches (typically spanning 50–100 mV from E_{corr}), intersected at E_{corr}. The anodic (b_a) and cathodic (b_c) Tafel slopes were obtained from the slopes of these linear regions on a semi-logarithmic current-density plot. The corrosion rate (CR) was calculated from i_{corr} using the standard Faradaic relationship:

$$CR\ (mm/year) = \left(i_{corr} \cdot \frac{M}{n \cdot F \cdot \rho}\right) \cdot 3.27 \cdot 10^{-3}, \qquad (1)$$

where M is the molar mass of iron (55.85 g/mol); $n = 2$ (electrons transferred); F is Faraday's constant (96485 C/mol); and ρ is the density of iron (7.87 g/cm³).

2.6.4. Calculation of inhibition efficiency

The inhibition efficiency ($IE\ (\%)$) of clove extract on mild steel corrosion in simulated seawater was determined using the following equation:

$$IE\ (\%) = \frac{I_{corr(b)} - I_{corr(i)}}{I_{corr(b)}}, \qquad (2)$$

where $I_{corr(b)}$ is the corrosion current density of the control (without inhibitor); $I_{corr(i)}$ is the corrosion current density in the presence of inhibitor; $IE\ (\%)$ is the inhibition efficiency.

2.6.5. Statistical analysis of data

All experimental measurements were performed in triplicate to ensure the reliability and the reproducibility of results. The mean values of corrosion potential (E_{corr}), corrosion current density (I_{corr}), and inhibition efficiency ($IE\ (\%)$) were calculated for each sample. Standard deviations were not reported in the tables due to the limited number of replicates; this is acknowledged as a limitation, and future work should include fuller statistical characterisation, including error bars and confidence intervals.

2.7. Electrochemical impedance spectroscopy (EIS)

EIS data were collected over a frequency range of 100 kHz to 10 mHz with a 10 mV AC perturbation, and spectra were fitted to equivalent circuit models using nonlinear least-squares methods as described by Barsoukov and Macdonald (2018), ensuring quality evaluation using χ^2 values, phase residuals, and confidence intervals [34].

2.8. Surface morphology

Surface morphology was previously carried out before immersion and afterwards (24 h) in simulated seawater with and without varying concentrations of clove oil extract (1.0, 2.0, and 3.0 mL/L) and evaluated using scanning electron microscopy (SEM), while energy-dispersive X-ray spectroscopy (EDS) provided elemental distributions and oxide/chloride surface characterisation,

performed in accordance with best practices for SEM/EDS-based corrosion analysis [35].

3. Results and discussions

3.1. Chemical analysis of the mild steel

The nominal chemical composition of the mild steel in weight percentage was: C (0.25 %), Mn (0.80 %), Si (0.28 %), P (≤ 0.04 %), S (≤ 0.05 %), and Fe balance, as presented in Table 1.

Table 1 – Chemical composition of ASTM A36 mild steel.

Element	Composition (wt. %)
C	0.25
Mn	0.80
Si	0.28
P	≤ 0.04
S	≤ 0.05
Fe	Balance

3.2. Fourier transform infrared analysis (FTIR) of clove essential oil

The FTIR spectrum of clove essential oil (Figure 1) revealed a rich array of characteristic absorption bands consistent with Syzygium aromaticum oil [18, 20]. These spectral features are in close agreement with previously reported FTIR fingerprints for clove essential oil and confirm the predominance of eugenol as the principal constituent [18, 22]. Crucially, the co-presence of oxygen-bearing functional groups (phenolic O–H and methoxy C–O–C), aromatic π-conjugated systems, and an electron-rich allyl moiety collectively provide the molecular prerequisites for effective adsorptive interaction with the mild steel surface through donation of lone-pair electrons and π-electrons to the electron-deficient *d*-orbitals of iron, thereby forming a stable surface-bound inhibitor film [19, 25].

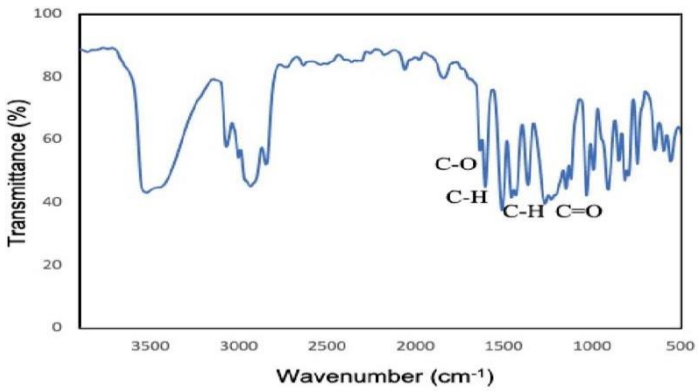


Figure 1 FTIR spectrum of a pure clove oil extract.

3.3. Open circuit potential (OCP) analysis

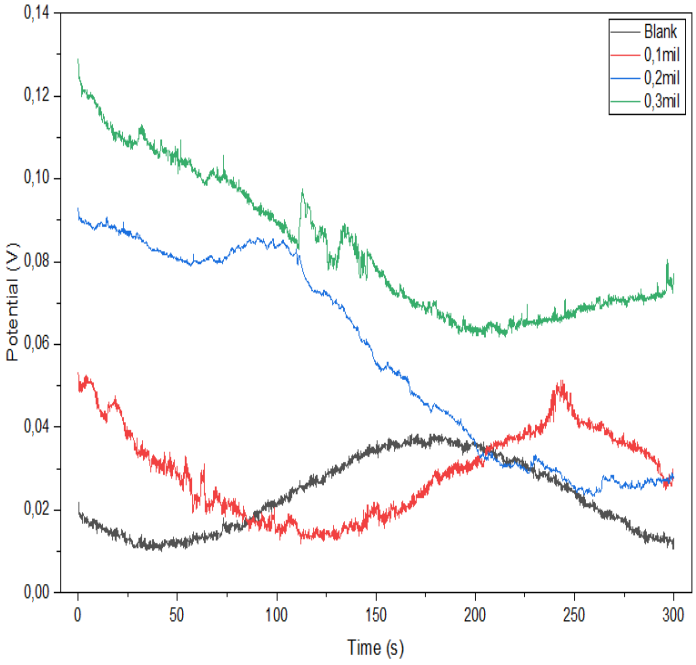


Figure 2 OCP graph of seawater with clove oil extract and control.

In the uninhibited simulated seawater, the OCP fluctuated irregularly between approximately 0.009 V and 0.039 V during the 300 s immersion. The observed instability and negative drift indicated continuous active dissolution of the mild steel surface due to the attack of chloride ions, which prevented the formation of a stable passive film. [38]. This behaviour is typical of an unprotected metal immersed in an aggressive chloride medium. With the introduction of 1.0 mL/L of clove extract, the OCP initially rose to about 0.05 V, but quickly decayed to below 0.03 V. The temporary positive shift implies partial adsorption of inhibitor molecules at the early stage; however, the unstable potential confirmed that the film was weak, non-uniform, or easily desorbed, offering limited inhibition. At 2.0 mL/L, the potential initially exhibited a value of around 0.09 V before gradually declining to approximately 0.025 V. Although this indicates partial surface coverage, the continued decay signifies that the film was not compact enough to fully protect the steel from chloride attack. The 3.0 mL/L concentration demonstrated the most stable and noble potential profile. The OCP started at about 0.125 V and stabilised around 0.07 V, which is substantially more positive than the other concentrations. The relative stability of this potential is consistent with the formation of a more adherent surface film compared to lower concentrations, suggesting greater inhibitor coverage, although complete passivation was not achieved within the 300 s monitoring window [7, 15].

3.4. Potentiodynamic polarisation (Tafel) analysis

The potentiodynamic polarisation (Tafel) curves obtained for mild steel in simulated seawater with and without clove essential oil are presented in Figure 3, and the corresponding electrochemical parameters are summarised in Table 2. The reported corrosion rates (on the order of 10^{-8} mm/year) are considerably lower than the typical values for mild steel in chloride media reported in the literature; this may reflect uncertainties in the Tafel extrapolation, particularly the difficulty of identifying unambiguous linear Tafel regions over a short polarisation window, and should be interpreted with caution. Independent gravimetric or solution analysis methods were not employed in this study to verify the corrosion rates, and this is identified as a limitation. In the uninhibited control, a corrosion potential (E_{corr}) of –0.627 V was recorded, with a corrosion current density (i_{corr}) of $2.287 \cdot 10^{-6}$ A/cm², anodic Tafel slope b_a = 130.8 mV/dec, cathodic Tafel slope b_c = 186.2 mV/dec, and a corrosion rate of $2.65 \cdot 10^{-8}$ mm/year. The addition of clove oil at all three concentrations resulted in a measurable reduction in i_{corr} and corrosion rate relative to the uninhibited control, confirming the inhibitory efficacy of the extract. At 1.0 mL/L clove oil, the i_{corr} decreased to $0.996 \cdot 10^{-6}$ A/cm², corresponding to an inhibition efficiency of 56.45 %, while at 3.0 mL/L the i_{corr} was further reduced to $0.887 \cdot 10^{-6}$ A/cm², yielding the highest inhibition efficiency of 61.22 % among the tested concentrations. The 2.0 mL/L concentration exhibited a markedly lower i_{corr} of $1.32 \cdot 10^{-6}$ A/cm² and the lowest inhibition efficiency of 42.27 %, which may reflect non-uniform inhibitor film coverage or competitive adsorption effects at this intermediate concentration [13]. The observed shifts in E_{corr} across all inhibitor concentrations were less than 85 mV relative to the control (ranging from –0.589 to –0.640 V), fulfilling the standard electrochemical criterion for classification of the clove oil as a mixed-type inhibitor, simultaneously suppressing both anodic iron dissolution and cathodic oxygen reduction reactions [9, 11]. This classification is further corroborated by the concomitant changes in both b_a and b_c values across all inhibitor concentrations: the anodic Tafel slopes increased slightly (from 130.8 to 112.5–134.5 mV/dec) while cathodic slopes showed more pronounced variation (186.2 to 153.2–228.0 mV/dec), indicating that while both electrode processes are retarded, the cathodic reaction is more substantially affected at higher concentrations [13, 23]. This pattern of mixed-type inhibition with cathodic emphasis at 3.0 mL/L is consistent with the behaviour previously reported for S. aromaticum essential oil in acidic media, where inhibition efficiencies of up to 94 % were attributed to the adsorption of eugenol and β-caryophyllene onto active steel surface sites through lone-pair electron and π-electron donation to the iron d-orbitals [25, 23]. The concentration-dependent inhibition observed, with 3.0 mL/L yielding the optimal efficiency of 61.22 %, is consistent with the general mechanistic principle that increasing inhibitor concentration promotes more complete monolayer coverage of the metal surface, progressively blocking active anodic and cathodic sites

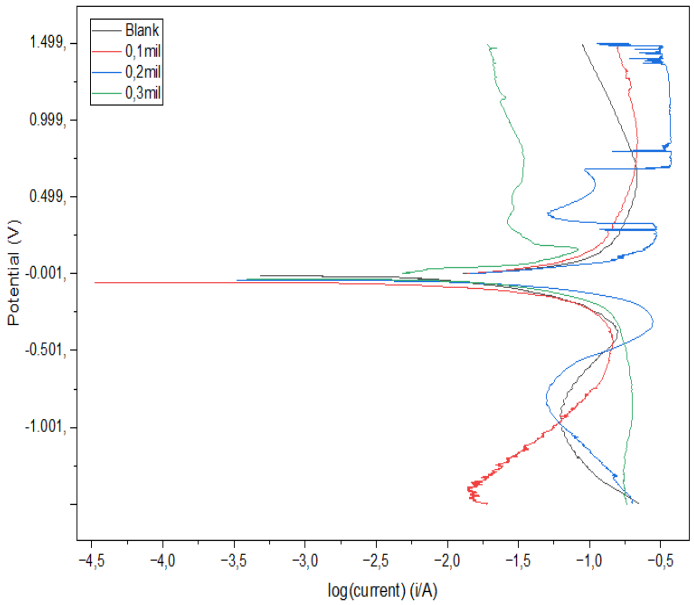


Figure 3 Tafel plots.

Table 2 – Potentiodynamic polarisation parameters for mild steel in simulated seawater with varying concentrations of clove oil extract.

Sample	E_{corr}, V	$i_{corr} \cdot 10^{-6}$, A/cm²	b_a, mV/dec	b_c, mV/dec	Efficiency, %	Corrosion rate, mm/year
Control	–0.627	2.287	130.8	186.2	–	$2.65 \cdot 10^{-8}$
1.0 mL/L Clove oil	–0.639	0.996	134.5	193.3	56.45	$1.16 \cdot 10^{-8}$
2.0 mL/L Clove oil	–0.640	$1.32 \cdot 10^{-6}$	134.1	228.0	42.27	$1.53 \cdot 10^{-8}$
3.0 mL/L Clove oil	–0.589	0.887	112.5	153.2	61.22	$1.03 \cdot 10^{-8}$

[11, 13]. The comparatively modest inhibition efficiencies relative to the values reported in acid media (HCl, H_2SO_4) are attributed to the near-neutral *p*H (~ 8.0) of simulated seawater, which limits the protonation of eugenol's nitrogen-free functional groups and reduces the electrostatic driving force for surface adsorption relative to the strongly acidic environments examined in prior studies [9, 12].

3.5. Electrochemical impedance spectroscopy (EIS) analysis

The electrochemical impedance spectroscopy (EIS) results are presented as Nyquist plots (Figure 4) and Bode plots (Figure 5). Nyquist plots for all systems displayed depressed capacitive semicircles over the examined frequency range, characteristic of a single time-constant behaviour arising from charge transfer at the mild steel/electrolyte interface in conjunction with double-layer capacitance [10, 14]. The depressed or non-ideal nature of the semicircles, commonly attributed to surface heterogeneity, roughness, and the distribution of relaxation times, was modelled using a constant phase element (CPE) in place of an ideal capacitor in the equivalent circuit [14]. The diameter of the capacitive semicircle, which is directly proportional to the charge transfer resistance (R_{ct}), increased progressively with increasing clove oil concentration relative to the control, providing direct impedimetric evidence of enhanced resistance to charge transfer at the inhibitor-coated steel surface [10, 24]. This enlargement of the Nyquist semicircle diameter with inhibitor addition confirms that the phytochemical constituents of clove oil, principally eugenol, adsorb onto the mild steel surface to form a resistive organic barrier layer that impedes the electrochemical corrosion reactions [10, 25]. The corresponding reduction in double-layer capacitance (C_{dl}) inferred from the impedance data is consistent with displacement of water molecules and adsorbed chloride ions from the steel surface by the organic inhibitor molecules, effectively reducing the dielectric constant of the interfacial layer and increasing its thickness [17, 24]. The Bode magnitude plots (Figure 5) showed a progressive increase in impedance modulus $|Z|$ at low frequencies with increasing clove oil concentration, with the 3.0 mL/L concentration exhibiting the highest low-frequency impedance, confirming superior protective film formation at this concentration [14, 17]. The Bode phase plots displayed a single broad phase angle maximum in the intermediate frequency range for all systems, consistent with the single time-constant behaviour observed in the Nyquist representation and confirming that the corrosion mechanism is governed by a charge transfer process across a resistive inhibitor film [10, 24]. The overall EIS results are in good concordance with the Tafel analysis, collectively identifying 3.0 mL/L as the optimal inhibitor concentration, and confirm the mixed-type inhibition mechanism of clove essential oil against mild steel corrosion in simulated seawater, consistent with the findings previously reported for eugenol-containing essential oils and plant extracts evaluated by EIS [14, 17].

The EIS data were fitted using a modified Randles circuit (Figure 6) comprising solution resistance (R_s), charge-transfer resistance (R_{ct}), and a constant phase element (Q) to account for surface heterogeneity:

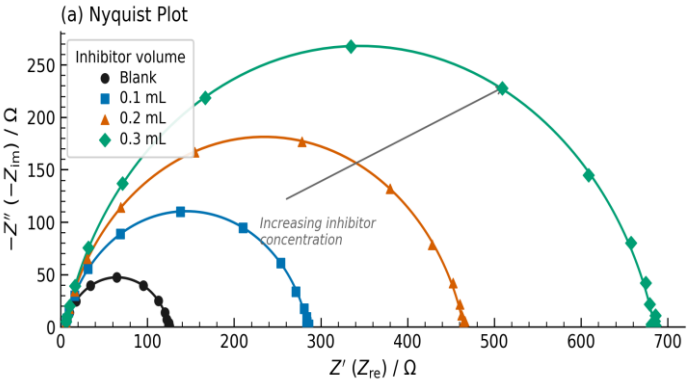


Figure 4 Nyquist plots.

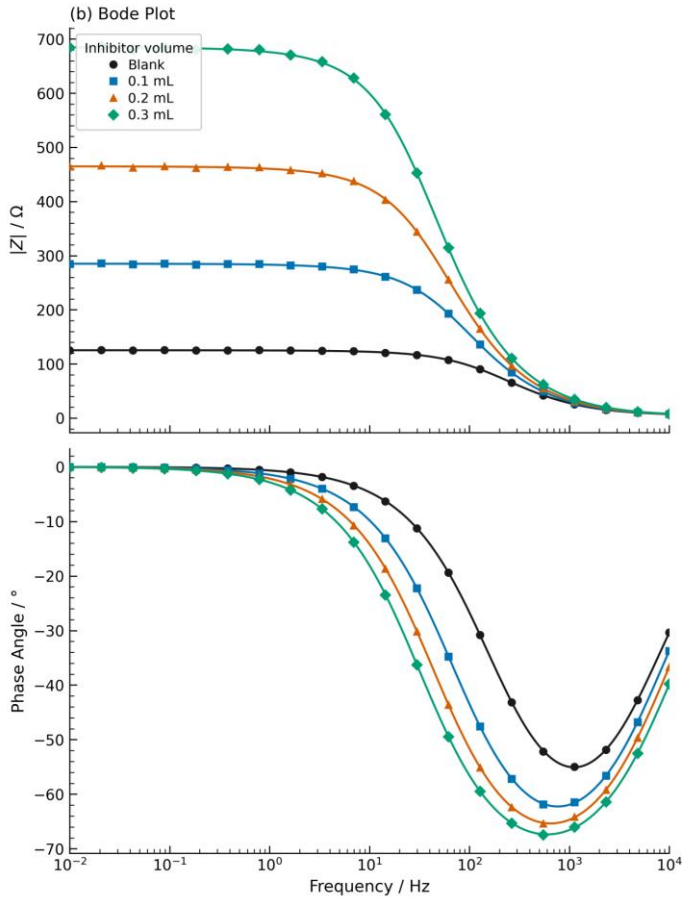


Figure 5 Bode plots.

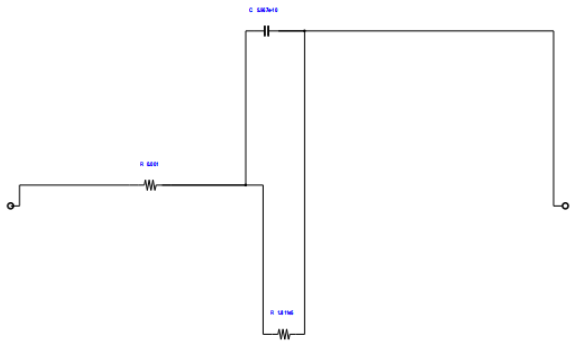


Figure 6 Equivalent circuit model (ECM) used to fit EIS data.

$$R_s(Q[R_{ct}]), \quad (3)$$

where R_s represents the solution resistance; Q(CPE) models the double-layer capacitance; and R_{ct} quantifies charge-transfer resistance. The depressed semicircles observed in all spectra confirm the non-ideal capacitive behaviour typical of organic inhibitor films. The significant increase in R_{ct} with inhibitor concentration indicates the formation of a dense, adherent barrier that effectively impedes charge transfer between the steel and the corrosive medium.

3.6. Surface morphology

3.6.1. Scanning electron microscopy and energy dispersive spectroscopy (SEM/EDS) – Control

The scanning electron micrographs of the mild steel surface after 24 hours of immersion in uninhibited simulated seawater are presented in Figures 7, 8, and 9 at 500x, 1000x, and 2000x magnification, respectively. At all magnification levels, the control steel surface displayed extensive and heterogeneous corrosion damage, characterised by the widespread deposition of voluminous, irregular corrosion product deposits, micro-pitting, and surface roughening attributable to the aggressive electrochemical attack by dissolved chloride ions, oxygen, and the saline electrolyte [4, 7]. The characteristic morphology of iron oxide and oxyhydroxide corrosion products – including amorphous $Fe(OH)_2$ and crystalline FeOOH phases – manifested as layered, nodular, and flaky deposits distributed across the steel surface, consistent with the classical mechanism of mild steel corrosion in marine environments [7, 8]. At higher magnification (2000x), micro-cracks within the corrosion product layer were discernible, indicative of the tensile stresses associated with volume expansion during the transformation of $Fe(OH)_2$ into the thermodynamically stable but voluminous Fe_2O_3 and Fe_3O_4 oxide phases [4, 8]. The EDS analysis of the control surface (Figure 10 and Table 3) revealed a composition

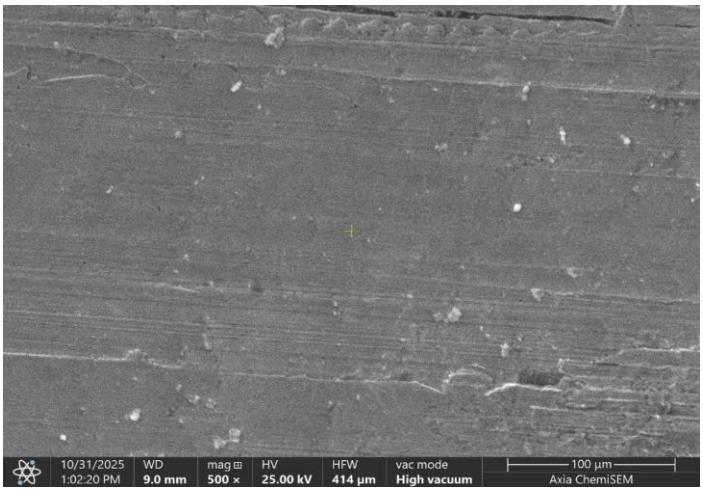


Figure 7 SEM diagram of the mild steel surface after 24 hours of immersion in simulated seawater without clove extract at 500x magnification.

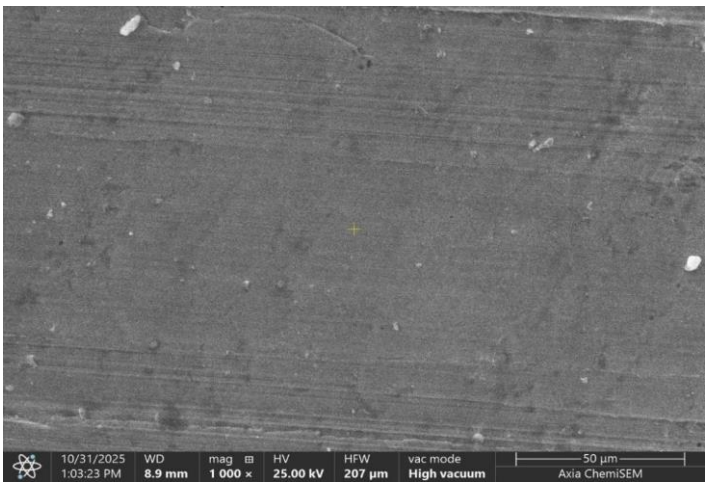


Figure 8 SEM diagram of the mild steel surface after 24 hours of immersion in simulated seawater without clove extract at 1000x magnification.

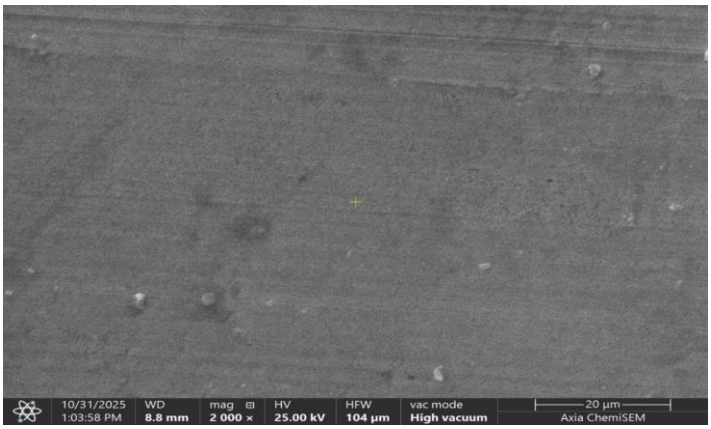


Figure 9 SEM diagram of the mild steel surface after 24 hours of immersion in simulated seawater without clove extract at 2000x magnification.

dominated by iron (Fe: 92.79 wt. %) with a significant oxygen content (O: 6.96 wt. %), the latter confirming the formation of iron oxide and hydroxide corrosion

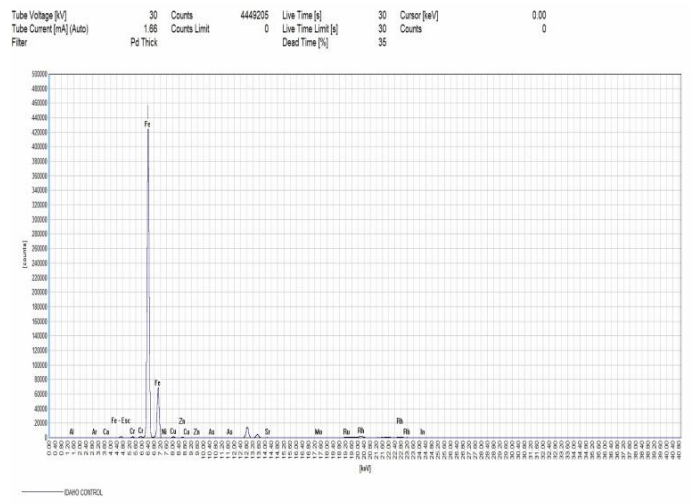


Figure 10 Energy dispersive X-ray spectroscopy (EDS) graph of the mild steel surface after 24 hours of immersion in simulated seawater.

Table 3 – Elemental composition (wt. %) from EDS analysis of the mild steel after 24 h of immersion in uninhibited simulated seawater.

Element	Control
Fe	92.79
Cr	0.25
Cl	0.00
Zn	0.00
Si	0.00
O	6.96
Total	100

products on the surface [7]. The low but non-negligible oxygen weight percentage in the control is consistent with the formation of a heterogeneous, non-protective corrosion product film, while trace chromium (Cr: 0.25 wt. %) reflects the minor alloying content of the mild steel substrate. The complete absence of chloride (Cl: 0.00 wt. %) in the EDS spectrum of the control is noteworthy and may indicate that chloride ions, despite being the principal aggressive species in the simulated seawater, were not retained within the surface corrosion product layer at detectable concentrations following the rinsing procedure, or that they participated primarily as catalysts for the passive film breakdown rather than as constituents of the corrosion product [4, 8].

3.6.2. Scanning electron microscopy and energy dispersive spectroscopy (SEM/EDS) – 1.0 mL/L

The SEM micrographs of the mild steel surface immersed in simulated seawater containing 1.0 mL/L of clove oil (Figures 11–13) revealed a surface morphology distinctly different from that of the uninhibited control, providing direct visual evidence of inhibitor adsorption and partial corrosion suppression. At 500x magnification (Figure 11), the surface exhibited a partial but incomplete organic film coverage with residual corrosion product deposits visible beneath and through the film, indicating that at this low concentration, inhibitor molecules do not achieve full monolayer coverage of the available metal surface area [25, 39]. At 1000x and 2000x magnification (Figures 12 and 13), a relatively discontinuous organic adsorption layer was observed, with some regions of the steel surface still displaying evidence of pitting and localised corrosion attack, consistent with the moderate inhibition efficiency of 56.45 % recorded from the Tafel analysis.

The EDS analysis (Figure 14 and Table 4) of the 1.0 mL/L-treated surface revealed several important compositional changes relative to the control: a reduction in iron content (Fe: 85.39 wt. % versus 92.79 wt. % for the control), accompanied by a substantial increase in oxygen content (O: 13.66 wt. % versus 6.96 wt. % for the control), and the appearance of measurable silicon (Si: 0.48 wt. %), zinc (Zn: 0.20 wt. %), and trace chloride (Cl: 0.07 wt. %) signals. The elevated oxygen content and reduced iron weight percentage are attributed to the deposition of organic oxygen-containing phytochemical molecules – principally eugenol, with its phenolic hydroxyl and methoxy functional groups – onto the steel surface, contributing to the observed oxygen signal [16, 39]. The detection of silicon likely reflects the incorporation of terpenoid-type phytoconstituents from the clove oil, while the trace chloride signal indicates incomplete exclusion of Cl^- ions from the surface at this lower inhibitor concentration, consistent with only partial surface coverage [16]. These EDS findings corroborate the electrochemical data in confirming that 0.1 mL of clove oil provides measurable but sub-optimal surface protection under the conditions examined.

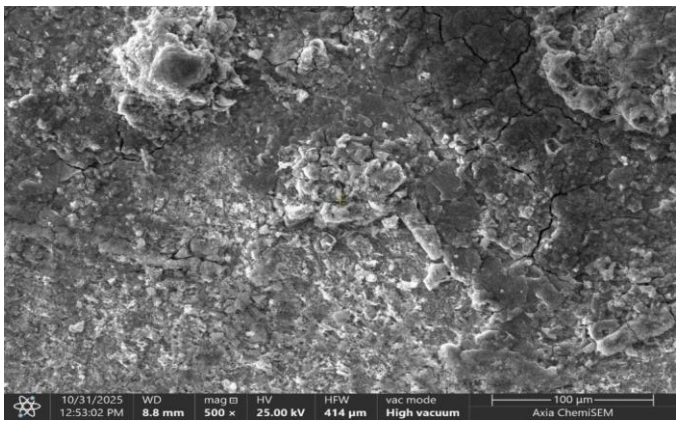


Figure 11 SEM diagram of the mild steel surface after 24 hours of immersion in simulated seawater + 1.0 mL/L clove extract at 500x magnification.

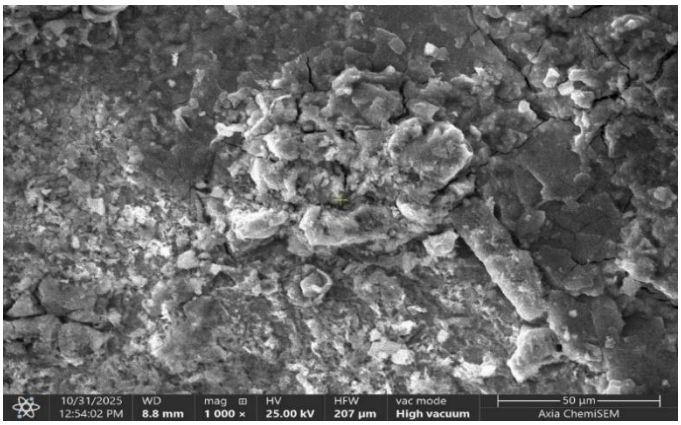


Figure 12 SEM diagram of the mild steel surface after 24 hours of immersion in simulated seawater + 1.0 mL/L clove extract at 1000x magnification.

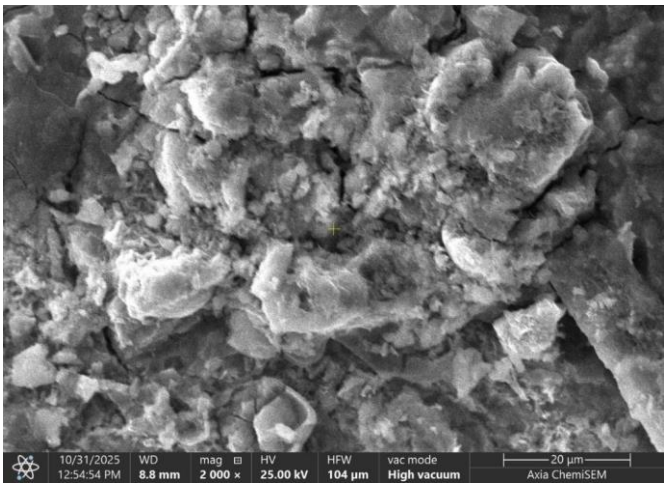


Figure 13 SEM diagram of the mild steel surface after 24 hours of immersion in simulated seawater at 2000x magnification + 1.0 mL/L clove extract at 2000x magnification.

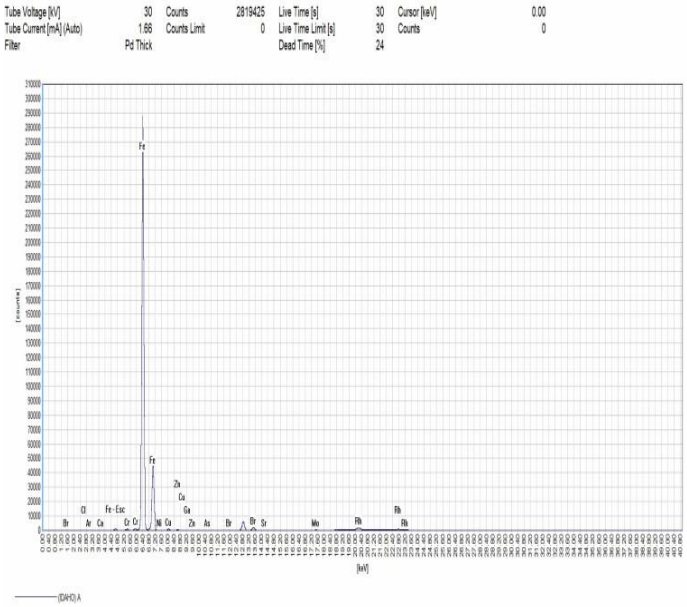


Figure 14 Energy dispersive X-ray spectroscopy (EDS) graph of the mild steel surface after 24 hours of immersion in simulated seawater with 1.0 mL/L of a clove extract.

Table 4 – Elemental composition (wt. %) from EDS analysis of mild steel after 24 h of immersion with 1.0 mL/L clove oil.

Element	1.0 mL/L
Fe	85.39
Cr	0.20
Cl	0.07
Zn	0.20
Si	0.48
O	13.66
Total	100

3.6.3. Scanning electron microscopy and energy dispersive spectroscopy (SEM/EDS) – 2.0 mL/L clove oil

The SEM micrographs obtained for the 2.0 mL/L clove oil treatment are shown in Figures 15–17. At 500x magnification (Figure 15), the steel surface appeared to bear a more uniform film deposit compared to the 1.0 mL/L treatment; however, irregularities, residual corrosion deposits, and localised pitting remained evident. At higher magnifications (Figures 16 and 17), the inhibitor film appeared partially developed, with regions of apparent organic deposition interspersed with zones of corrosion product accumulation [13, 39]. The observed surface heterogeneity at 2.0 mL/L is consistent with the anomalously low inhibition efficiency of 42.27 % recorded from the Tafel analysis at this concentration – lower than that of the 1.0 mL/L treatment – confirmed that at this intermediate concentration, the inhibitor adsorption layer may be less compact or stable than at lower or higher concentrations, possibly due to competitive adsorption phenomena or reorganisation of the adsorbed phytochemical film at the electrode surface [13, 21]. The EDS analysis (Figure 18 and Table 5) of the 0.2 mL-treated surface showed a composition closely

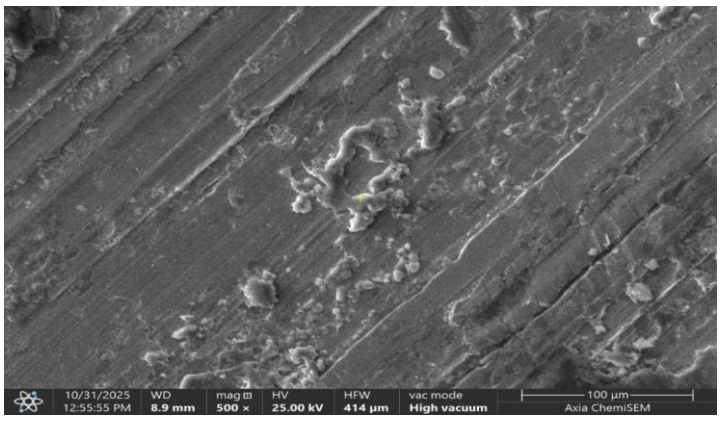


Figure 15 SEM diagram of the mild steel surface after 24 hours of immersion in simulated seawater + 2.0 mL/L clove oil extract at 500x magnification.

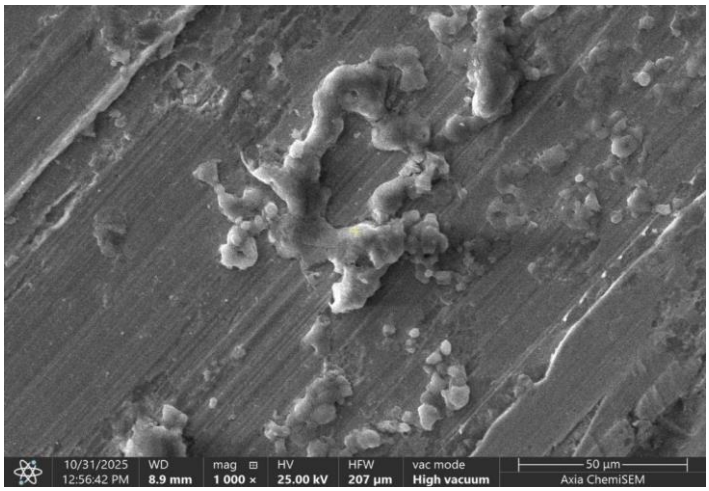


Figure 16 SEM diagram of the mild steel surface after 24 hours of immersion in simulated seawater + 2.0 mL/L clove oil extract at 1000x magnification.

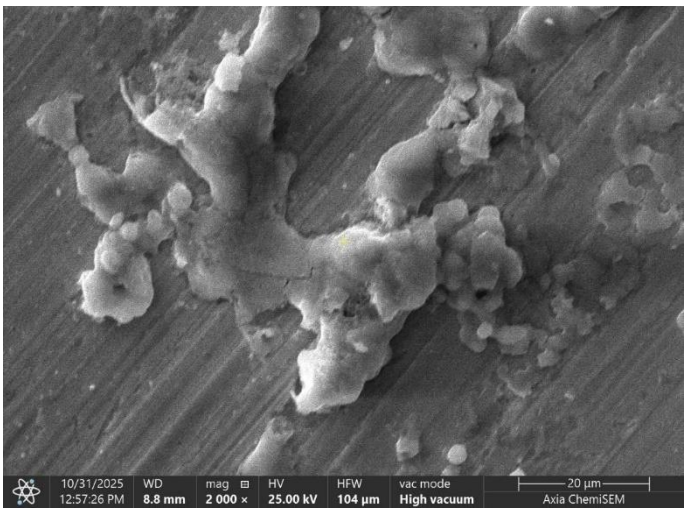


Figure 17 SEM diagram of the mild steel surface after 24 hours of immersion in simulated seawater + 2.0 mL/L clove oil extract at 2000x magnification.

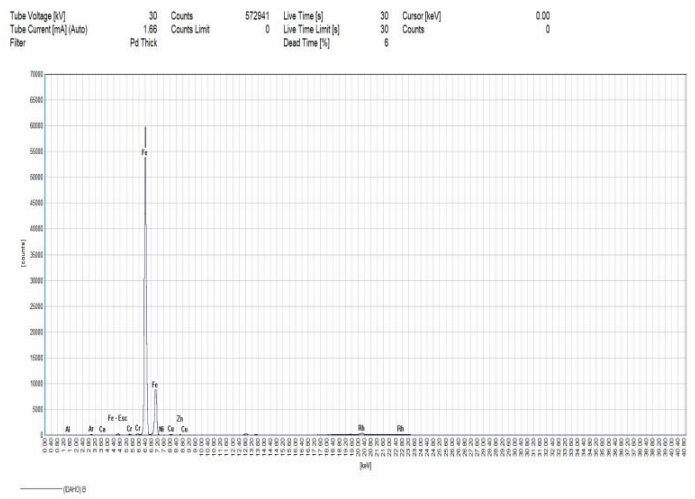


Figure 18 Energy dispersive X-ray spectroscopy (EDS) graph of the mild steel surface after 24 hours of immersion in simulated seawater with 2.0 mL/L of clove oil extract.

Table 5 – Elemental composition (wt. %) from the EDS analysis of mild steel after 24 h of immersion with 2.0 mL/L clove oil.

Element	2.0 mL/L
Fe	92.20
Cr	0.27
Cl	0.00
Zn	0.00
Si	0.00
O	7.53
Total	100

resembling that of the uninhibited control: Fe: 92.20 wt. %, O: 7.53 wt. %, with no detectable Cl, Zn, or Si. The near-control-level iron content and the relatively low oxygen signal confirm that the protective organic film formed at 2.0 mL/L is thin and provides limited elemental differentiation from the base steel, which may in part account for the reduced electrochemical protection observed at this concentration [21, 39]. The absence of Si and Zn signals, in contrast to the 1.0 mL/L treatment, may reflect the nature and distribution of the phytochemical constituents adsorbed at this concentration, with the dominant eugenol component forming a thin but uniform layer that does not significantly alter the bulk EDS signal relative to the substrate [16].

3.6.4. Scanning electron microscopy and energy dispersive spectroscopy (SEM/EDS) – 3.0 mL/L clove oil

The SEM micrographs of the mild steel surface treated with 0.3 mL of clove oil (Figures 19–21) exhibited the most significantly altered and protected surface morphology among all tested conditions, providing compelling visual corroboration of the superior electrochemical protection at this concentration. At 500x magnification (Figure 19), the steel surface displayed a markedly smoother and more uniform covered appearance relative to the control and lower-concentration treatments, with the characteristic rough corrosion product deposits of the uninhibited surface substantially attenuated, indicative of the formation of a more complete, compact organic adsorption film [25, 39]. At 1000x and 2000x magnifications (Figures 20–21), the inhibitor film exhibited a relatively continuous morphology with significantly reduced micro-pitting and surface roughness, consistent with more complete monolayer coverage of the steel surface by eugenol and associated phytochemical molecules at this higher concentration [5, 39]. The suppression of corrosion product deposit morphology at 3.0 mL/L corroborates the highest inhibition efficiency of 61.22 % and the lowest

corrosion current density (i_{corr} = 0.887 · 10⁻⁶ A/cm²) observed in the Tafel analysis, confirming that increasing inhibitor concentration promotes more extensive surface coverage and more effective barrier film formation [13].

The EDS analysis (Figure 22 and Table 6) of the 3.0 mL/L-treated surface revealed an elemental composition intermediate between the control and the 1.0 mL/L-treatment: Fe: 88.58 wt. %, O: 11.21 wt. %, Cr: 0.21 wt. %, with no detectable Cl, Zn, or Si. The elevated oxygen content (11.21 wt. %) relative to the control (6.96 wt. %) confirms the deposition of oxygen-rich organic phytochemical inhibitor molecules – particularly eugenol – onto the steel surface, and the complete absence of chloride in the EDS spectrum at 0.3 mL indicates the effective exclusion of aggressive Cl^- ions from the inhibitor-covered surface, demonstrating the protective efficacy of the adsorbed organic film [5, 7, 16]. The progressive increase in the surface oxygen content from control (6.96 %) to 3.0 mL/L (11.21 %), with the 1.0 mL/L

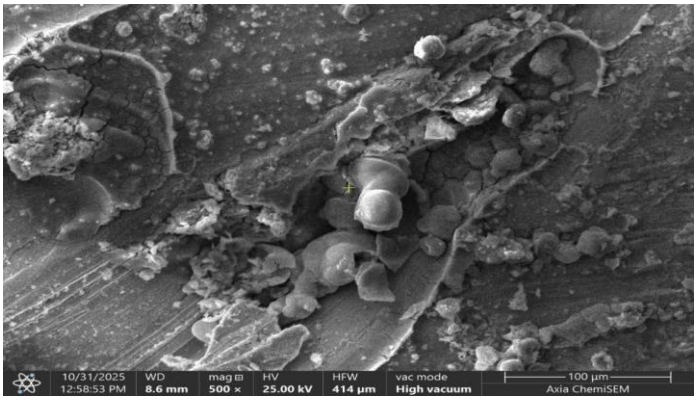


Figure 19 SEM diagram of the mild steel surface after 24 hours of immersion in simulated seawater + 3.0 mL/L clove oil extract at 500x magnification.

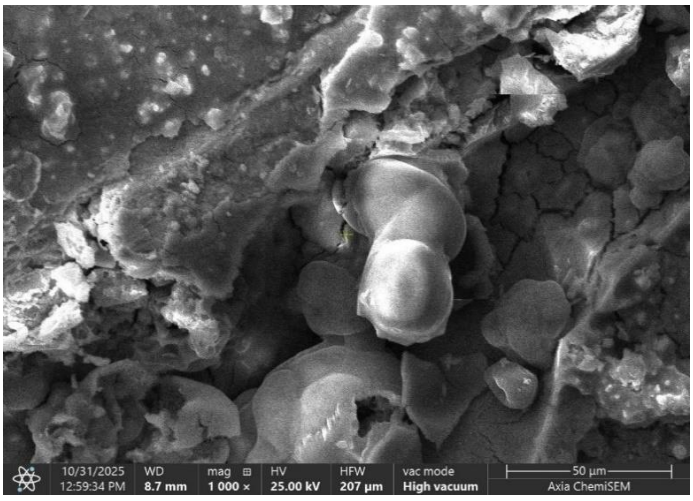


Figure 20 SEM diagram of the mild steel surface after 24 hours of immersion in simulated seawater + 3.0 mL/L clove oil extract at 1000x magnification.

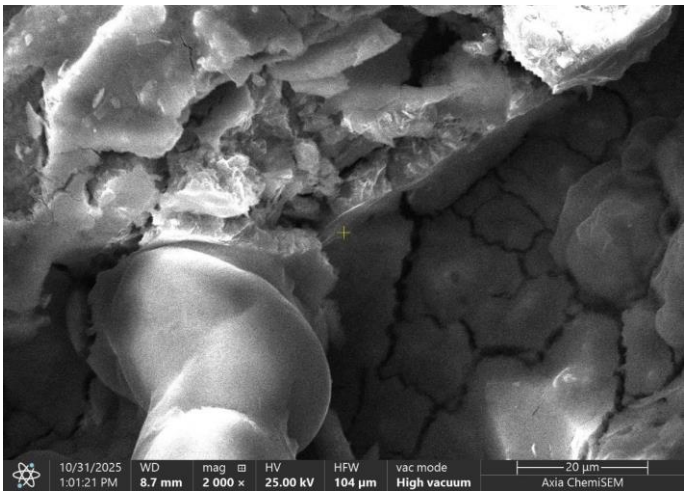


Figure 21 SEM diagram of the mild steel surface after 24 hours of immersion in simulated seawater + 3.0 mL/L clove oil extract at 2000x magnification.

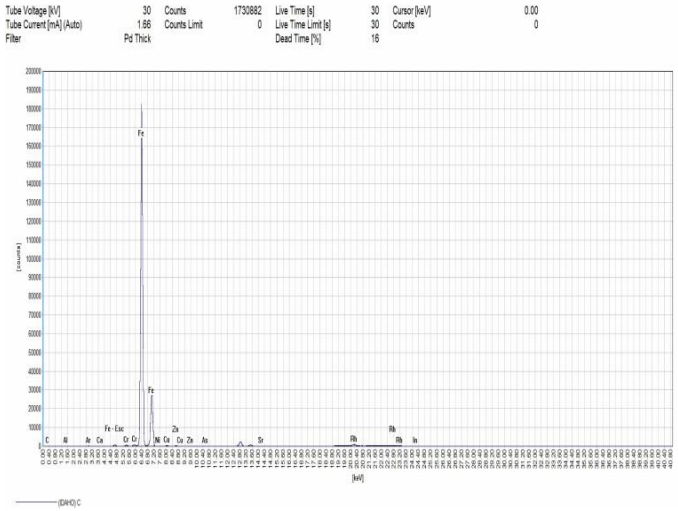


Figure 22 Energy dispersive X-ray spectroscopy (EDS) graph of the mild steel surface after 24 hours of immersion in simulated seawater with 3.0 mL/L of clove oil extract.

Table 6 – Elemental composition (wt. %) from EDS analysis of mild steel after 24 h of immersion with 3.0 mL/L of clove oil.

Element	3.0 mL/L
Fe	88.58
Cr	0.21
Cl	0.00
Zn	0.00
Si	0.00
O	11.21
Total	100

treatment exhibiting the highest oxygen signal (13.66 %), likely reflects a combination of increased organic film deposition and differing oxide/hydroxide corrosion product formation at each condition, with the 1.0 mL/L

surface exhibiting a mixed organic–inorganic film composition and the 3.0 mL/L surface bearing a denser, more purely organic phytochemical protective layer [5, 16].

4. Conclusions

This study evaluated clove essential oil (Syzygium aromaticum) as a green corrosion inhibitor for mild steel in simulated seawater (3.5 wt. % NaCl) using FTIR spectroscopy, OCP monitoring, potentiodynamic polarisation, EIS, and SEM-EDS. FTIR confirmed that eugenol is the dominant active constituent, with its phenolic O–H, methoxy C–O–C, aromatic π-system, and allyl C=C functionalities providing the molecular basis for chemisorptive electron donation to the iron d-orbitals, forming a stable protective surface film. All electrochemical techniques consistently identified 3.0 mL/L as the optimal inhibitor concentration, yielding the highest inhibition efficiency of 61.22 %, the lowest i_{corr} ($0.887 \cdot 10^{-6}$ A/cm^2), and the greatest charge transfer resistance. OCP and Tafel analyses classified the extract as a mixed-type inhibitor – simultaneously retarding anodic iron dissolution and cathodic oxygen reduction – based on E_{corr} displacements within ± 85 mV of the control across all concentrations. EIS Nyquist and Bode plots confirmed a concentration-dependent increase in impedance modulus and charge transfer resistance, consistent with the progressive formation of a resistive organic barrier layer. SEM micrographs corroborated these findings, showing markedly reduced corrosion product deposition and surface roughness at 3.0 mL/L, while EDS analysis confirmed an elevated surface oxygen content (11.21 wt. % versus 6.96 wt. % for the control) and complete exclusion of Cl^- ions, confirming effective inhibitor film coverage. The anomalous inhibition efficiency of 42.27 % at 2.0 mL/L is attributed to competitive adsorption effects and reduced film compactness at this intermediate concentration. Moderate overall efficiencies relative to studies in acidic media reflect the reduced electrostatic adsorption driving force at a near-neutral *p*H (~ 8.0) of seawater. These results establish clove essential oil as a promising biorenewable corrosion inhibitor under simulated seawater conditions, with future work recommended to include quantum chemical modelling, molecular dynamics simulations, and temperature-dependent adsorption isotherm studies to fully elucidate the inhibition thermodynamics.

Supplementary materials

No supplementary materials are available.

Funding

This research had no external funding.

Acknowledgments

None.

Author contributions

Maureen Olere Oisakede: Conceptualization; Data curation; Formal Analysis; Supervision; Writing – Review & Editing.

Blessed Osayemwen Enagbonma: Investigation; Methodology; Project administration; Writing – Original draft; Resources; Software; Validation; Visualization.

George Ochuko Emoghene: Investigation; Methodology; Project administration; Writing – Original draft; Resources; Software; Validation; Visualization.

Judith Efionayi: Investigation; Methodology; Project administration; Writing – Original draft; Resources; Software; Validation; Visualization.

Great Chukwudaro Onyejerue: Investigation; Methodology; Project administration; Writing – Original draft; Resources; Software; Validation; Visualization.

Conflict of interest

The authors declare no conflict of interest.

Additional information

Maureen Olere Oisakede, Scopus ID: 58967548600; ORCID: 0000-0002-3906-0460; ResearchGate: https://www.researchgate.net/profile/Maureen-Oisakede; LinkedIn: https://www.linkedin.com/in/maureen-oisakede-ph-d; Google Scholar: https://scholar.google.com/citations?hl=en&user=0s6MjJoAAAAJ.

References

1. El-Sherik AM. Trends in oil and gas corrosion research and technologies: production and transmission. 1st ed. Woodhead Publishing: Sawston, Cambridge, United Kingdom; 2017. 882 p.

2. NACE International, International measures of prevention, application, and economics of corrosion technologies study, 2016.

3. AkzoNobel Interpon, The cost of corrosion report, AkzoNobel Powder Coatings Ltd., 2025.

4. Kassinis C, Aresti L, Koronides M, Christodoulides P, et al., A review on the environment's influence on coastal marine steel corrosion and *in-situ* monitoring, Journal of Materials Science: Materials in Engineering, **20(3)** (2025) 125. https://doi.org/10.1186/s40712-025-00352-2

5. Liu P, Microbially influenced corrosion of steel in marine environments: A review from mechanisms to prevention, Microorganisms, **11(9)** (2023) 2299. https://doi.org/10.3390/microorganisms11092299

6. Melchers RE, Jeffrey R, Chaves IA, Petersen RB, Predicting corrosion for life estimation of coastal steel infrastructure, Materials and Corrosion, **76(6)** (2025) 776–789. https://doi.org/10.1002/maco.202314201

7. Pusparizkita YM, Fardilah VA, Aslan C, Jamari J, Bayuseno AP, Understanding low-carbon steel marine corrosion through simulation in artificial seawater, AIMS Materials Science, **10(3)** (2023) 499–516. https://doi.org/10.3934/matersci.2023028

8. Mazilu A, Benea L, Axente ER, Monitoring and evaluation of the corrosion behavior in seawater of the low-alloy steels BVDH36 and LRAH36, International Journal of Molecular Sciences, **25(12)** (2024) 6405. https://doi.org/10.3390/ijms25126405

9. Pourmohseni M, Rashidi A, Karimkhani M, Preparation of corrosion inhibitor from natural plant for mild stil immersed in an acidic environmental: experimental and theoretical study, Scientific Reports, **14(1)** (2024) 7937. https://doi.org/10.1038/s41598-024-58637-z

10. Al-Moubaraki AH, Chaouiki A, Alahmari JM, Al-hammadi WA, et al., Development of natural plant extracts as sustainable inhibitors for efficient protection of mild steel: Experimental and first-principles multi-level computational methods, Materials, **15(23)** (2022) 8688. https://doi.org/10.3390/ma15238688

11. Thacker H, Ram V, Green corrosion inhibitors derived from plant extracts and drugs for mild steel in acid media: A review, Results in Surfaces and Interfaces, **18** (2025) 100364. https://doi.org/10.1016/j.rsurfi.2024.100364

12. Tidke SD, Kulkarni SS, Marathe AC, Comprehensive review of green corrosion inhibitors for safe and sustainable protection of mild steel in acidic environments, Discover Electrochemistry, **2** (2025) 40, https://doi.org/10.1007/s44373-025-00055-5

13. Holla BR, Mahesh R, Manjunath HR, Anjanapura VR, Plant extracts as green corrosion inhibitors for different kinds of steel: A review, Heliyon, **10(14)** (2024) e33748. https://doi.org/10.1016/j.heliyon.2024.e33748

14. Rizi A, Sedik A, Acidi A, Rachedi KO, et al., Sustainable and green corrosion inhibition of mild steel: Insights from electrochemical and computational approaches, ACS Omega, **8(49)** (2023) 47224–47238. https://doi.org/10.1021/acsomega.3c06548

15. Shathani P, Ogunmuyiwa EN, Obadele BA, Oluseyi OP, Plant leaf extracts as green corrosion inhibitors of steel in acidic and seawater environments: a review, Environmental Science and Pollution Research, **32(51)** (2025) 28954–28975. https://doi.org/10.1007/s11356-025-37116-6

16. Bandeira RM, Lima FP, Nunes MS, dos Santos EC, et al., The green plant-based corrosion inhibitors – a sustainable strategy for corrosion protection, Surface Science and Technology, **3** (2025) 19. https://doi.org/10.1007/s44251-025-00084-7

17. Fazal BR, Becker T., Kinsella B, Lepkova K, A review of plant extracts as green corrosion inhibitors for CO_2 corrosion of carbon steel, npj Materials Degradation, **6** (2022) 5. https://doi.org/10.1038/s41529-021-00201-5

18. Anissa A, Sedik A, Rizi A, Bouasla R, et al., Examination of the main chemical components of essential oil of *Syzygium aromaticum* as a corrosion inhibitor on the mild steel in 0.5 M HCl medium, Journal of Molecular Liquids, **391(B)** (2023) 123423. https://doi.org/10.1016/j.molliq.2023.123423

19. Rebbah B, Haib AE, Lahmady S, Forsal I, et al., Synthesis, characterization, and inhibition effects of a novel eugenol derivative bearing pyrrole functionalities on the corrosion of mild steel in a HCl acid solution, RSC Advances, **14** (2024) 14152–14160. https://doi.org/10.1039/D4RA01337A

20. Haro-González JN, Castillo-Herrera GA, Martínez-Velázquez M, Espinosa-Andrews H, Clove essential oil (*Syzygium aromaticum* L. Myrtaceae): Extraction, chemical composition, food applications, and essential bioactivity for human health, Molecules, **26(21)** (2021) 6387. https://doi.org/10.3390/molecules26216387

21. Ahamad J, Characterization of essential oil composition of *Syzygium aromaticum Linn*. (Clove) by GC-MS and evaluation of its antioxidant activity, Journal of Angiotherapy, **7(1)** (2023) 1–5. https://doi.org/10.25163/angiotherapy.719358

22. Ahamad J, Omer AY, Majid DA, Khidr TM., Jameel SY, Essential oil characterization in clove (Syzygium aromaticum Linn.) by GC-MS and detection of its adulteration by ATR-FTIR method, Applied Biological Research, **24(3)** (2022) 309–316. https://doi.org/10.5958/0974-4517.2022.00037.4

23. Chaieb E, Bouyanzer A, Hammouti B, Benkaddour M, Inhibition of the corrosion of steel in 1 M HCl by eugenol derivatives, Applied Surface Science, **246(1–3)** (2005) 199–206. https://doi.org/10.1016/j.apsusc.2004.11.011

24. Seddik NB, Achache M, Zarki Y, Elmourabit M, et al., Combining theoretical and experimental studies on the effective protection of brass in 3 % NaCl medium by loading extracted eugenol corrosion inhibitor into an organoclay, Chemistry Africa, **8** (2025) 723–740. https://doi.org/10.1007/s42250-024-01152-5

25. Ngadiwiyana N, Gunawan G, Ismiyarto I, Prasetya NBA, et al., Harnessing the power of clove (*Syzygium aromaticum*): polymerized eugenol as bio-based solution for corrosion resistance and antimicrobial coatings, Polymer Bulletin, **83** (2026) 100. https://doi.org/10.1007/s00289-025-06110-w

26. Jones DA. Principles and prevention of corrosion. 2nd ed. Prentice Hall: Upper Saddle River, NJ; 1996. 592 p.

27. Revie RW, Uhlig HH. Corrosion and corrosion control. 4th ed. Wiley: Hoboken, NJ; 2008. 430 p.

28. ASTM D1141-98, Standard Practice for the Preparation of Substitute Ocean Water, Annual Book of ASTM Standards, Philadelphia, 2004.

29. Pavia DL, Lampman GM, Kriz GS, Vyvyan JR. Introduction to spectroscopy. 4th ed. Cengage Learning: Boston, MA; 2014. 784 p.

30. Rodríguez JDW, Gastaldi E, Ruiz T, Rigou P, et al., Rapid ATR-FTIR method for monitoring the release of major components of clove essential oil encapsulated into a complex organic matrix, In book: Flavour Science - Proceedings of the XV Weurman Flavour Research Symposium Publisher: Verlag der Technischen Universität Graz, (2018) 499–502. https://doi.org/10.3217/978-3-85125-593-5-106

31. Orazem ME, Tribollet B. Electrochemical impedance spectroscopy (The ECS series of texts and monographs). 2nd ed. Wiley: Hoboken, NJ; 2017. 768 p.

32. El-Sayed NH, Corrosion inhibition of carbon steel in chloride solutions by some amino acids, European Journal of Chemistry, **7(1)** (2016) 14–18. https://doi.org/10.5155/eurjchem.7.1.14-18.1331

33. Verma C, Ebenso EE, Quraishi MA, Corrosion inhibitors for ferrous and non-ferrous metals and alloys in ionic sodium chloride solutions: A review, Journal of Molecular Liquids, **248** (2017) 927–942. https://doi.org/10.1016/j.molliq.2017.10.094

34. Barsoukov E, Macdonald JR. Impedance spectroscopy: theory, experiment, and applications. 3rd ed. Wiley: Hoboken, NJ; 2018. 534 p.

35. Goldstein J, Newbury DE, Michael JR, Ritchie NWM, Scanning electron microscopy and X-ray microanalysis. 4th ed. Springer: New York, NY; 2018. 573 p.

36. Umoren SA, Solomon MM, Synergistic corrosion inhibition effect of metal cations and mixtures of organic compounds: A Review, Journal of Environmental Chemical Engineering, **5(1)** (2017) 246–273. https://doi.org/10.1016/j.jece.2016.12.001

37. Abdel-Gaber AM, Khamis E, Abo-ElDahab H, Adeel Sh, Inhibition of aluminium corrosion in alkaline solutions using natural compound, Materials Chemistry and Physics, **109(2–3)** (2008) 297–305. https://doi.org/10.1016/j.matchemphys.2007.11.038

38. Chohan IM, Ahmad A, Sallih N, Bheel N, et al., Effect of seawater salinity, pH, and temperature on external corrosion behavior and microhardness of offshore oil and gas pipeline: RSM modelling and optimization, Scientific Reports, **14** (2024) 16543. https://doi.org/10.1038/s41598-024-67463-2

39. Furtado LB, Nascimento RC, Guimarães MJOC, Brasil SLDC, et al., Green eugenol oligomers as corrosion inhibitors for carbon steel in 1 M HCl, Materials Research, **25** (2022). https://doi.org/10.1590/1980-5373-mr-2022-0012